Send Orders for Reprints to reprints@benthamscience.net

Design and Development of Microemulsion Based Transdermal Gel of Lercanidipine Hydrochloride by Assimilation of Rotatable Central Composite Design and Principal Component Analysis

Anjali Dhingani*[1], Jaydeep Patel[1], Kevin Garala[1] and Abhay Dharamsi[2]

[1]*Department of Pharmaceutics, Atmiya Institute of Pharmacy, Kalawad Road, Rajkot, Gujarat, India;* [2]*Department of Pharmaceutics, Maliba Pharmacy College, Surat, Gujarat, India*

Abstract: The objective of the present research was to design and develop microemulsion (ME) based transdermal systems of poorly water soluble drug, Lercanidipine hydrochloride (LDPH) by assimilation of central composite design and principal component analysis (PCA) as two important paradigms of quality by design. LDPH loaded O/W MEs were optimized with amounts of oil (Capryol 90), surfactants mixture (Cremophor EL and Ethanol) and water as independent variables along with cumulative amount of drug permeated in 24 h (Q_{24}), flux (J_{ss}) and lag time (t_L) as dependent variables. The optimized batch of LDPH loaded ME was successfully converted into microemulsion based gel (MBG) for increased patient compliance. The results of *in vitro* skin permeation of the optimized batch of LDPH loaded MBG revealed significant increase in permeability parameters as compared to its convention formulation. The values of J_{ss} for optimized batch of LDPH loaded MBGs (196.47 μg/cm^{2}h) revealed 7.95 cm^2 area requirement to obtain the desired input rate of LDPH within 24 h application. All these concluded suitability of experimental design and PCA for design and development of O/W type MEs as carriers for transdermal delivery of poorly water soluble drug, LDPH.

Keywords: Central composite design, lercanidipine hydrochloride, microemulsion, principal component analysis, quality by design, transdermal drug delivery.

1. INTRODUCTION

Lercanidipine hydrochloride (LPDH) is a calcium channel blocker used for the treatment of angina that belongs to class II of biopharmaceutical classification system (BCS) with extensive first-pass metabolism and absolute oral bioavailability of about 10%. The short biological half-life (2-5 h) and high value of log P (6.0) condensed LDPH as an ideal candidate for transdermal drug delivery system (TDDS) in order to achieve its therapeutic levels [1-6]. TDDS is targeted towards achievement of systemic levels of drugs which possess high hepatic first pass metabolism. In TDDS, the drug molecule passes through the various layers of the skin and reaches the systemic circulation in order to produce its therapeutic effect. Although transdermal route is an attractive alternative to oral and hypodermic administration, limited numbers of drugs are available as transdermal products. This is due to the barrier function primarily by the stratum corneum (SC) layer of the skin. Consequently, the entry of therapeutic agents becomes difficult due to the relatively impermeable nature of the skin [7, 8]. To overcome this limitation, novel drug delivery systems like microemulsion, nanoparticles and vesicular systems are currently being cast-off by the investigators to expedite drug transportation through the skin [9, 10]. In the last few years, microemulsions (MEs) have received increasing courtesy because of their potential advantages such as enhanced drug solubility, thermodynamic stability and increased drug permeation rate [11-13]. The Quality by Design (QbD) paradigm underlying pharmaceutical drug product development relies on multivariate data, both from formulation and the process in order to explain the multi-factorial relationship between formulation variables, process variables and drug product attributes. Design of experiment (DoE), risk assessment, principal component analysis (PCA) and process analytical technology (PAT) are the major tools that can be used in QbD process as and when necessary. The majority of scientists now routinely use DoE as a part of scientific approach in order to reduce costs and improve quality within timelines to obtain robust products and processes [14, 15]. In light of these, the aim of present investigation was to design and develop O/W type MEs for transdermal delivery of antihypertensive drug LDPH using QbD approaches.

2. MATERIALS AND METHODS

2.1. Materials

LDPH was obtained as a gift sample from Torrent Research Center, Gandhinagar, India. The materials like; Capmul MCM, Capmul PG8, Captex 355, Acconon CC-6, Capmul GMO50, Capmul PGE 860, Caprol ET and Capmul MCM C8 were generously donated by Abitec Corporation, USA. Miglyol 812 and Imwitor 742 were kindly gifted from Sasol GmbH, Witten, Germany. Capryol 90, Labrafac CC, Labrafac Lipophile WL1349, Labrafil M 2125CS, Maisine 35-1 and Paceol were gifted from Gettefosse Saint-Priest Cedex, France. Sefsol 218 was obtained as a gift sample from Nikko Chemicals, Tokyo, Japan. Cremophor RH40,

*Address correspondence to this author at the Department of Pharmaceutics, Atmiya Institute of Pharmacy, Kalawad Road, Rajkot-360005, Gujarat, India; Tel: +919723533919, Fax: +912812563766;
E-mail: anjali.patel27@gmail.com

2211-7393/13 $58.00+.00

Gelucire 44/14, Lauroglycol 90 and Solutol HS 15 were donated from BASF Corporation, USA. Other Chemicals like Tween 20, Tween 40, Tween 60, Tween 80, Polyethylene Glycol (PEG) 400, Propylene Glycol (PG) and Sodium alginate were purchased from Himedia Labs, Mumbai, India whereas Span 40, Span 60, Span 80, Isopropyl alcohol (IPA), n-butanol, Ethanol, White wax, Xanthan gum and Cetosteryl alcohol were procured from SD Fine Chem, Mumbai, India. Isopropyl Myristate (IPM), Olive oil, Oleic acid, Castor oil, Magnesium stearate, Titanium dioxide, Zinc oxide and Colloidal silica were procured from Loba Chem, Mumbai, India. Double distilled water was used throughout the study.

2.2. Selection of Microemulsion Components

2.2.1. Selection of oil (Solubility Studies)

The solubility of LDPH was measured in numerous oils by shake flask method. An excess amount of drug was introduced into 2 mL of each oil and these mixtures were sealed in glass vials. Each of the sample was vortexed (GeNei, Bangalore, India) for 5 min to facilitate initial mixing. Further, vials were charged on an environmental shaker bath (Tempo Instruments and Equipments Pvt. Ltd., Mumbai, India) for a period of 72 h at 37°C with 300 rpm speed. Each vial was centrifuged at 10000 rpm for 10 min using a high speed centrifuge (Remi Laboratory Instruments, Mumbai, India). The amount of drug in all samples was determined by their subsequent dilution with pH 7.4 phosphate buffer containing 30% v/v PEG 400 using double beam UV Visible spectrophotometer (UV-1700, Shimadzu Corporation, Tokyo, Japan) against blank at 353 nm. The study was repeated in triplicate and their mean values were documented [16, 17].

2.2.2. Selection of Surfactant (Emulsification Study)

For each surfactant, 10 mL of 10% w/v solution was prepared in distilled water and previously optimized oil was subsequently added to each of these solutions with an increment of 10 µL along with vortexing until the systems become cloudy [18-20].

2.2.3. Selection of Cosurfactant (Emulsification Study)

Five cosurfactants were screened for their potential to assist previously selected surfactant in terms of emulsification oil phase. The screening of cosurfactant was done on the basis of amount of oil emulsified [18-20].

2.3. Selection of Surfactant and Cosurfactant Ratio (K_m)

The surfactant and cosurfactant ratio was optimized by constructing pseudo ternary phase diagrams with various ratios (1:3, 1:2, 1:1, 2:1, 3:1) by water titration method. Diverse combinations of oil and S_{mix} in weight ratios of 1:9, 1:8, 1:7, 1:6, 1:5, 1:4, 1:3, 1:2, 1:1, 2:3, 3:7, 3:2, 7:3, 4:1 and 9:1) were titrated by distilled water (aqueous phase) to delineate all boundaries of phases precisely formed. The pseudo-ternary phase diagram with highest microemulsion area was selected as optimized ratio of surfactant to cosurfactant for all further trials (Fig. **1**) [18-20].

2.4. Preparation of Drug Loaded MEs

Drug loaded MEs were prepared by dissolving fixed amount of LDPH (1% w/w) in optimized oil phase with subsequent addition of optimized surfactant and cosurfactant blend (S_{mix}) since in the present study it was previously decided that 1 mL or 1 g of final formulation would be most suitable for the *in vitro* permeation study of ME or MBG, respectively. Hence, as per the dosage information available in the literatures (10 mg) we have formulated 1% w/w loaded ME. The resultant mixtures were continuously stirred for a period of 2 min on vortex mixer. The aqueous phase (distilled water) was further added slowly with continuous stirring using high speed homogenizer (Remi Laboratory Instruments, Mumbai, India) [21-23].

2.5. Optimization

A five level three factor rotatable central composite design ($\alpha = 1.68$) was employed to evaluate influence of independent variables [amount of oil (X_1), amount of surfactant mixture (surfactant and cosurfactant - X_2) and amount of water (X_3)] on critical quality attributes. The design consisted of eight factorial points, six axial points and one center points with total 15 runs (LDPH-ME-F1 to LDPH-ME-F15) (Table **1**) in total. A second order quadratic model incorporating interactive and polynomial terms was used to evaluate responses [24-26].

$$Y_i = b_0 + b_1X_1 + b_2X_2 + b_3X_3 + b_{12}X_{12} + b_{13}X_{13} + b_{23}X_{23} + b_{11}X^2_1 + b_{22}X^2_2 + b_{33}X^2_3 \quad (1)$$

Critical responses were identified amongst all restrained evaluation parameters by PCA using a trial version of Unscrambler® 10.2 (CAMO AS, Norway, Switzerland) [27, 28]. Data were further analyzed by Microsoft Excel® version 2010 (Microsoft corporation, Washington, USA) for regression analysis. Analysis of variance (ANOVA) study was executed to assure nonsignificant difference between full developed model and reduced model. Contour and response surface plots were generated to study response variations against independent variables using Sigma Plot® software [29, 30].

2.6. Evaluation Parameters of Drug Loaded MEs

2.6.1. Globule Size and Size Distribution

All the batches of LDPH loaded MEs were subjected to measurement of globule size and size distribution immediately after preparation. The samples were analyzed by particle size analyzer (Zetatrac, U2552, New York, USA) at 25°C with an angle of 90° [21, 22].

2.6.2. Zeta Potential (ζ)

The zeta potentials (ζ) of all the batches of LDPH loaded MEs were determined by the particle size analyzer [24].

2.6.3. Refractive Index (RI)

The RI values of all the batches of LDPH loaded MEs were determined using refractometer (Bausch and Lomb Optical Company, Rochester, NY, USA) [31].

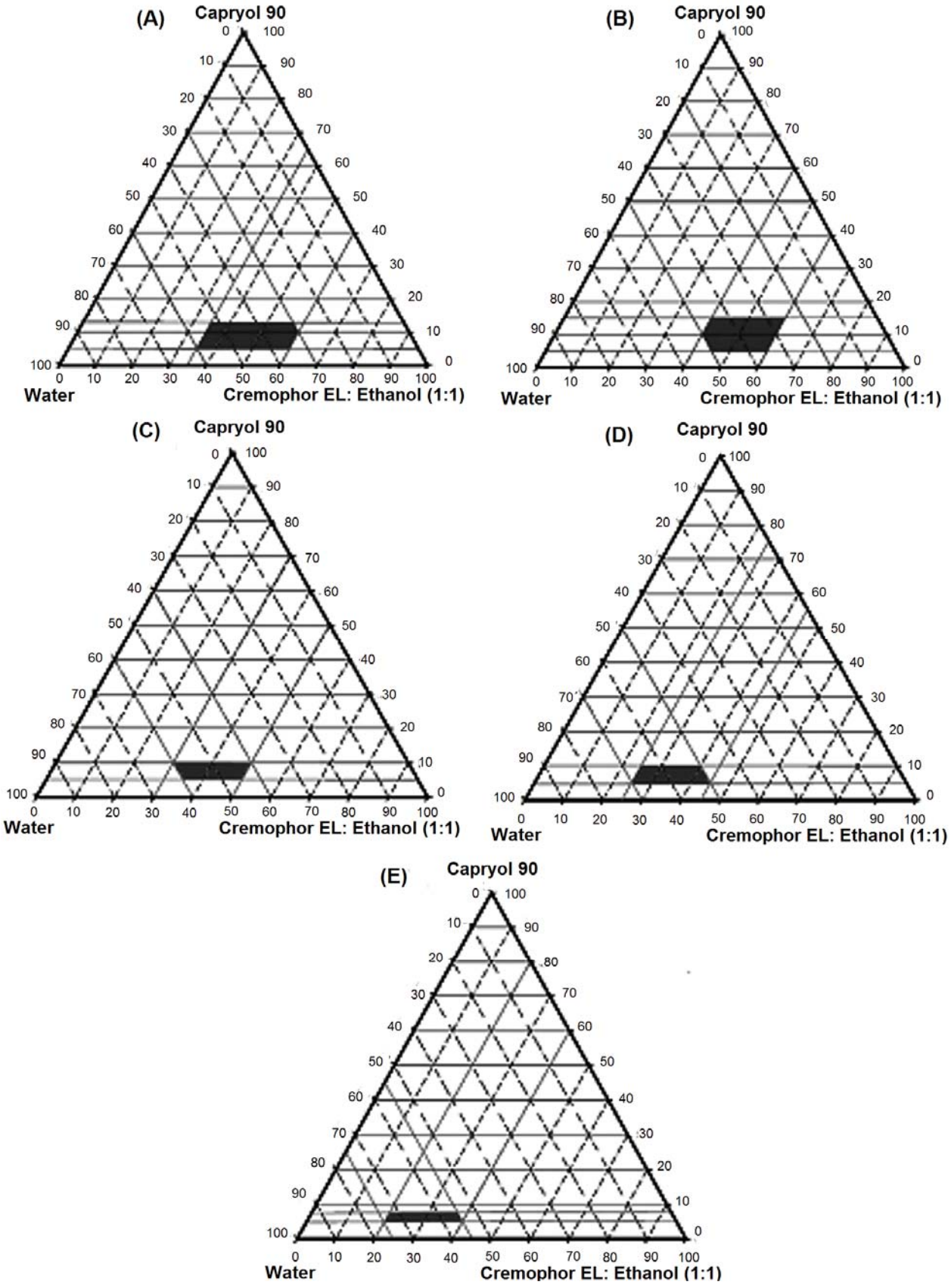

Fig. (1). Pseudo-ternary phase diagrams with different ratios of S_{mix} (**A**) 3:1, (**B**) 2:1, (**C**) 1:1, (**D**) 1:2, (**E**) 1:3 for LDPH loaded MEs.

Table 1. Design Layout of Box-Behnken Design Batches for LDPH Loaded MEs.

Batch Code	Transformed Values		
	X_1[a]	X_2[b]	X_3[c]
LDPH-ME-F1	-1	-1	-1
LDPH-ME-F2	1	-1	-1
LDPH-ME-F3	-1	1	-1
LDPH-ME-F4	1	1	-1
LDPH-ME-F5	-1	-1	1
LDPH-ME-F6	1	-1	1
LDPH-ME-F7	-1	1	1
LDPH-ME-F8	1	1	1
LDPH-ME-F9	-1.68	0	0
LDPH-ME-F10	1.68	0	0
LDPH-ME-F11	0	-1.68	0
LDPH-ME-F12	0	1.68	0
LDPH-ME-F13	0	0	-1.68
LDPH-ME-F14	0	0	1.68
LDPH-ME-F15	0	0	0
Coded Values	**Actual Values (mL)**		
	X_1[a]	X_2[b]	X_3[c]
-1.68	5	40	20
-1	7.02	44.05	26.07
0	10	50	35
1	12.98	55.95	43.93
1.68	15	60	50

[a] X_1: Amount of oil (Capryol 90), [b] X_2: Amount of surfactant [Cremophor EL: Ethanol (2:1)], [c] X_3: Amount of water.

2.6.4. Percentage Transmittance (%T)

The percent transmittances of all the batches of LDPH loaded MEs were measured by subjecting each sample to UV spectrophotometer at 650 nm using distilled water as a blank [31].

2.6.5. Percentage Drug Content (% DC)

Accurately weighed samples of LDPH loaded MEs were dissolved individually in 10 mL of methanol and stirred by vortex mixer for a period of 10 min. Each of the solution was filtered, using membrane filter (0.45 μm) and the drug content of each filtrate was estimated spectrophotometrically against blank at 353 nm [31].

2.6.6. Viscosity

The viscosities of all the batches of LDPH loaded MEs were determined by using rheometer (Brookfield Engineering Laboratories, Inc., Middleboro, MA) with S62 spindle and 25°C temperature in triplicates [32].

2.6.7. In vitro Permeation Study

The *in vitro* skin permeation studies were carried out under the guideline compiled by Committee for the Purpose of Control and Supervision of Experiments on Animal (CPCSEA, Ministry of Culture, Government of India) and all the study protocols were approved by the Local Institutional Animal Ethics Committee of Atmiya Institute of Pharmacy, Rajkot, Gujarat, India (CPCSEA No.:1004/9O/Q/06//CPCSEA/ PG-1005, Dated: 10/01/2012) [31-34]. Rat abdominal skin was mounted with the SC facing opposite to the receptor compartment on the Franz diffusion cell (Orchid scientific, Nasik, India) containing a diffusion area of 1.77 cm^2. The receptor compartment was filled with 16 mL of pH 7.4 phosphate buffer containing 30% v/v PEG 400 and the content was magnetically stirred. The donor compartment was filled with 1 mL of LDPH loaded ME to achieve desired drug concentration at the site [21-23]. Parameters such as, flux, permeability coefficient (K_p) and enhancement ratio (ER) were also calculated as per following equations.

$$J_{ss} = \frac{dM}{dt} \quad (2)$$

where, M was the cumulative amount of drug permeated (mg) through skin per unit area (cm^2) within experimental time t (h). Other parameters such as, permeability coefficient (K_p) and enhancement ratio (ER) were also calculated according to the following equations.

$$K_p = \frac{J_{ss}}{C_{donor}} \quad (3)$$

$$ER = \frac{\text{Flux from microemulsion formulation}}{\text{Flux from drug solution}} \quad (4)$$

where, J_{ss} was the flux, C_{donor} was the total amount of drug in donor compartment, h was the thickness of skin sample and t_L was the lag time.Further, in order to quantify the drug concentration in the skin (drug retained in skin) after permeation study, donor solutions were removed and the skin was washed twice with distilled water before unclamping from diffusion cells [35-37].

2.6.8. Thermodynamic Stability

The optimized batch of LDPH loaded ME was subjected to different thermodynamic stability tests to assess their physical stability. All samples were evaluated in terms of phase separation at the end of analysis. Six cycles between refrigerator temperature (2-8°C) and 45°C with storage at each temperature not less than 48 h were conducted [21-23].

2.6.9. Tranmission Electron Microscopy

The optimized batch of LDPH loaded ME was subjected to transmission electron microscope (H-7000, Hitachi, Ibaraki, Japan) in order to estimate globule morphology. Briefly, LDPH loaded ME was plunged for 10-15 min on a coated carbon grid stained with 2% uranyl acetate solution. The samples were subsequently washed with fresh distilled water before analysis. Radiation generated at 200 kV was utilized as X-Ray source with camera length of 100 cm. Two dimensions of X-Ray patterns were photographed for each sample studied [21-23].

2.7. Preparation of Drug Loaded Microemulsion Based Gels (MBGs)

An amount of drug representing 1% w/w for LDPH loaded ME was added to an optimized amount of oil phase, consisting of the optimized quantities of surfactant and co-surfactant. Pre-optimized amount of thickening agent was dispersed in water by using high speed homogenizer at 1000 rpm. The previously prepared drug loaded non-aqueous part was added slowly to this aqueous dispersion under magnetic stirring. Various thickening agents, namely, sodium alginate, xanthan gum, hydroxypropyl methylcellulose (Methocel K4M), Polaxomer 188 and Carbopol 940 were evaluated for their ability to thicken drug loaded MEs. The optimized thickening agent was further evaluated for the effect of its concentrations [38-40].

2.8. Evaluation Parameters of Drug Loaded MBGs

2.8.1. Appearance

All the batches of LDPH loaded MBGs were evaluated visually for their color, homogeneity, consistency and phase separation [38-40].

2.8.2. Globule Size and Size Distribution

The optimized batch of LDPH loaded MBG was diluted (100 times) with purified water and endangered to the measurement of globule size and size distribution immediately [38-40].

2.8.3. Zeta Potential (ζ)

The zeta potential (ζ) of optimized batch of LDPH loaded MBG was determined by the particle size analyzer after their dilution (100 times) with purified water [38-40].

2.8.4. pH

The pH of all the batches of LDPH loaded MBGs were measured by digital pH meter. Each of samples was subjected to 100 times dilution by purified water before analysis [38-40].

2.8.5. Viscosity

The viscosities of all the batches of LDPH loaded MBGs were determined by using rheometer with S61 spindle and 25°C temperature in triplicates [41].

2.8.6. Percentage Drug Content (% DC)

Accurately weighed amount (1 g) of the optimized batch of LDPH loaded MBG was transferred in a 100 mL volumetric flask and the volume was made up to the mark with methanol. Subsequently, the solution was filtered, using membrane filter (0.45 µm) and the drug content of filtrate was estimated spectrophotometrically against blank using spectrophotometer at 353 nm [40].

2.8.7. In vitro Permeation Study

Rat abdominal skin was mounted with the SC facing opposite to the receptor compartment on the Franz diffusion cell containing a diffusion area of 1.77 cm^2. The receptor compartment was filled with 16 mL of pH 7.4 phosphate buffer containing 30% v/v of PEG 400 and the content was magnetically stirred at 300 rpm to prevent stagnant layer formation. The donor compartment was filled with 1 g of optimized batch of LDPH loaded MBG to achieve desired drug concentration at the site [38-41].

2.8.8. Skin Irritation Study

Twelve different rats were randomly divided into two groups as test and reference for skin irritation study of optimized MBG of LDPH. The optimized batch of LDPH loaded MBG was applied to the dorsal surface of one group of rats as test and 0.8% v/v aqueous solution of formaldehyde was applied to another group of rats as reference. Each rat was evaluated for any sign of erythema or edema over a period of 48 h according to Draize scoring method [42]. The primary dermal irritation index (PDII) was calculated by adding the average erythema and edema scores for the 1 h, 12 h, 24 h and 48 h scoring intervals and dividing by the number of evaluation intervals [43].

2.8.9. Stability Study

The optimized batch of LDPH loaded MBG was subjected to stability study as per International Conference on Harmonization (ICH) guidelines. The sample was filled in a 10 g collapsible aluminum tubes and stored at 40±2°C/75±5% RH over a period of 6 months in a stability chamber (Remi Electrotechnik Ltd. Mumbai, India). At predetermined time intervals samples were evaluated statistically [44].

3. RESULTS AND DISCUSSION

3.1. Selection of Microemulsion Components

3.1.1. Screening of Oil

In the present study, selection of oil for the preparation of MEs was done on the basis of their propensity to solubilize maximum amount of drug [45]. Maximum solubility of LDPH (97.13 mg/mL) was observed in Capryol 90 which was significantly higher compared to water (0.48 mg/m). Hence, O/W type ME was decided to develop for transdermal administration of LDPH (Table **2**) [10, 46].

3.1.2. Screening of Surfactant

In the present study, nonionic surfactants were selected since they are known to be less affected by pH change, generally regarded as safe and are biocompatible. The surfactant screening was done on the basis of their emulsification potential which was measured in terms of the amount of oil emulsified by each surfactant. The results of emulsification study optimized oil phase (Capryol 90) by hydrophilic surfactants depicted highest emulsification potential of Cremophor EL than all other hydrophilic surfactants studied (Table **2**).

3.1.3. Screening of Cosurfactant

The data clearly illustrated that Capryol 90 undewent highest emulsification with ethanol as cosurfactant (Table **2**). This explained the importance of cosurfactant addition to MEs [45].

3.2. Optimization of Surfactant and Cosurfactant Ratio (K_m)

The data depicted decrease in microemulsification region with decrease in surfactant concentrations with respect to cosurfactant and hence the study was limited to 1:3 K_m ratio. Similarly there was a significant increase in the microemulsification region with increase in the amount of surfactant upto 2:1 K_m ratio [20]. The optimized phase diagram of LDPH loaded MEs had largest microemulsification region with oil concentration 5-15% w/w, S_{mix} concentration 40-60% w/w and water concentration 20-50% w/w.

3.3. Optimization

Thus, the present study was persisted with Central Composite design (Rotatable) for optimization of LDPH loaded MEs using of oil, surfactant mix (S_{mix}) and water as three critical factors followed by PCA to scrutinize critical responses

Table 2. Solubility of LDPH in Various Oils and Emulsification of Optimized oil by Surfactants and Cosurfactants.

Oils	Solubility (mg/mL)	Surfactants[a]	Amount of Oil Emulsified (µL)
Capmul MCM	81.13 ± 5.34	Cremophor EL	550.00 ± 30.65
Capmul PG8	55.24 ± 3.66	Cremophor RH40	466.67 ± 28.26
Captex 355	12.46 ± 1.32	Caprol PGE 860	116.67 ± 6.12
Capryol 90	97.13 ± 5.67	Gelucire 44/14	216.67 ± 12.45
Labrafac CC	37.65 ± 2.35	Solutol HS15	150.00 ± 10.34
Labrafac Lipophile WL 1349	46.14 ± 3.45	Tween 20	433.33 ± 20.45
Labrafil M 2125 CS	44.13 ± 3.33	Tween 40	240.33 ± 11.67
Maisine 35-1	87.57 ± 5.45	Tween 60	258.67 ± 12.45
Imwitor 742	33.15 ± 2.12	Tween 80	333.33 ± 11.78
Miglyol 812	24.9 ± 1.57	**Cosurfactants**	**Amount of Oil Emulsified (µL)**
IPM	34.67 ± 3.67	PEG 400	90.34 ± 1.23
Paceol	72.06 ± 5.52	PG	88.21 ± 1.09
Sefsol 218	90.12 ± 6.33	IPA	94.12 ± 1.03
Oleic acid	20.33 ± 1.44	n-Butanol	97.35 ± 1.19
Olive oil	10.24 ± 1.23	Ethanol	100.34 ± 0.57
Castor oil	12.54 ± 1.16		

The results are of mean ± SD (n=3); [a] 10% v/v surfactant.

(quality attributes) among all parameters studied. The actual value of each of the selected factor has been summarized against their respective coded values in Table **1**. The results of responses like globule size, polydispersibility index (PI), zeta potential (ζ), refractive index (RI), percentage transmittance (%T), percentage drug content (%DC), viscosity (η), cumulative amount of drug permeated after 24 h (Q_{24}), flux (J_{ss}), lag time (t_L), enhancement ratio (ER), permeability coefficient (K_p) and drug retained in skin (DRS) for experimental design batches of LDPH loaded MEs have been summarized in Table **3** [47-49]. As depicted in Fig. **2**(**A**), first principal component (PC1) was responsible for 64% of the total variance in the data set and second (PC2) was responsible for a further 30% [50]. A graphical display of the result of agglomerative hierarchy cluster analysis (AHCA) is shown in Fig. **2**(**B**) as dendrogram which was used for evaluation of similarity and dissimilarity of all design batches [51]. The results of dendrogram demonstrated clustering of all formulations into five major groups; group I (F5), group II (F8, F9, F10 and F6), group III (F7, F12 and F1), group IV (F11, F15 and F4) and group V (F14, F13, F3 and F2). Further, all the five groups were found to be relatively distant and substantially different from one another. Clusters of all formulations were correlated by PCA score plot in a similar way (Fig. **2**(**C**)). Correlation loading plot was constructed to decide most important variables for further optimization. The results scrutinized Q_{24}, J_{ss} and t_L as three critical responses on the basis of their retention between two eclipses of correlation loading plot (Fig. **2**(**D**)). Plotting the eigenvalues against corresponding PC, produces a scree plot that illustrates the rate of change in the magnitude of eigenvalues which are based on inspection of correlation matrix eigenvalues. The scree plot for LDPH loaded MEs (Fig. **2**(**E**)) illustrated that the eigenvalues for each component were in descending order. All other components (PC3 to PC15) which appeared after the break were assumed to be trivial and hence removed from the study. The equations representing the quantitative effect of the formulation variables on the measured responses are shown below. The polynomial equations could be used to draw conclusions after considering the magnitude of coefficients and their mathematical sign.

$$Q_{24}\ (Y_1) = 4140.63 + 63.6X_1 + 456.13X_2 + 107.21X_3 + 4.87X_1X_2 + 25.2X_1X_3 - 15.79X_2X_3 - 176.74X_1^2 - 140.47X_2^2 - 65.34X_3^2 \quad (5)$$

$$J_{ss}\ (Y_2) = 187.04 + 3.48X_1 + 24.40X_2 + 3.21X_3 - 0.31X_1X_2 - 0.43X_1X_3 + 0.29X_2X_3 - 7.75X_1^2 - 2.26X_2^2 - 3.05X_3^2 \quad (6)$$

$$t_L\ (Y_3) = 0.4606 - 0.0218X_1 - 0.1215X_2 - 0.01X_3 - 0.0113X_1X_2 - 0.0062X_1X_3 - 0.0012X_2X_3 + 0.0027X_1^2 + 0.0045X_2^2 - 0.0079X_3^2 \quad (7)$$

For Q_{24} (Y_1), coefficients b_{12}, b_{13}, b_{23} and b_{33}; for J_{ss} (Y_2), coefficients b_{12}, b_{13}, b_{23} and b_{22} whereas for t_L (Y_3) coefficients b_3, b_{12}, b_{13}, b_{23}, b_{11}, b_{22} and b_{33} were found to be insignificant ($P > 0.05$) and hence, they were separated from full model to develop a reduced model. The removal of insignificant terms was further justified by executing analysis of variance (ANOVA) test. The high value of correlation coefficients for Q_{24} (Y_1), J_{ss} (Y_2) and t_L (Y_3) illustrated goodness of fit. The critical values of F for Y_1 and Y_2 were found to be 5.19 (df = 4, 5) whereas for Y_3 it was found to be 4.88 (df = 7, 5). For all three responses, calculated F values [0.6187 (Y_1), 1.0234 (Y_2) and 0.8367 (Y_3)] were less than their respective critical values which supported nonsignificant difference between full and reduced models. The data of all the 15 batches of experimental design were used to generate interpolated values with the assistance of response surface and contour plots. The final reduced model equations for all three responses could be summarized as;

$$Q_{24}\ (Y_1) = 4007.18 + 63.6X_1 + 456.13X_2 + 107.21X_3 - 170.12X_1^2 - 129.84X_2^2 \quad (8)$$

$$J_{ss}\ (Y_2) = 182.41 + 3.47X_1 + 24.4X_2 + 3.2X_3 - 7.34X_1^2 - 2.64X_3^2 \quad (9)$$

$$t_L\ (Y_3) = 0.46 - 0.0217X_1 - 0.1215X_2 \quad (10)$$

3.3.1. Influence of Formulation Factors on Q_{24} (Y_1)

The highest value of Q_{24} (4512.14 μg/cm^2) was observed with batch LDPH-ME-F12 (Table **3**). Moreover, response surface and contour plots (Fig. **3**(**i**)) for Y_1 also illustrated strong influence of all three factors (oil, S_{mix} and water) studied. The data of regression analysis revealed positive value for coefficients b_1, b_2 and b_3 which indicated that Q_{24} was increased with increasing oil, S_{mix} and/or water concentration. This might be attributed to reduction in globule size of MEs with increase in amount of oil, membrane disturbing potential of surfactant (cremophor EL) and cosurfactant (ethanol) and enhanced hydrophilicity of the highly lipidic drug by water phase [16-19].

3.3.2. Influence of Formulation Composition Factors on J_{ss} (Y_2)

The flux (J_{ss}) of all experimental design batches was also strongly influenced by all three independent variables (oil, S_{mix} and water) with a highest value of 220.34 μg/cm^{2}h for batch LDPH-ME-F12 (Table **3**). In addition to these, response surface and contour plots (Fig. **3**(**ii**)) for Y_2 also exemplified strong influence of all three variables studied. The data of regression analysis revealed positive value for coefficients b_1, b_2 and b_3 which indicated that J_{ss} was increased with increasing oil, S_{mix} and/or water concentration. This might be attributed to reduction in globule size of MEs with increase in amount of oil, membrane disturbing potential of surfactant and cosurfactant and enhanced hydrophilicity of the highly lipidic drug by water phase [16-19].

3.3.3. Influence of Formulation Factors on t_L (Y_3)

Lag time was highly influenced by all three independent variables studied with lowest t_L value of 0.27 h for batch LDPH-ME-F12 (Table **3**). Moreover, response surface and contour plots (Fig. **3**(**iii**)) for Y_3 also illustrated strong influence of three factors (oil, S_{mix} and water) analyzed. The data of regression analysis revealed negative value of b_1 and b_2 coefficients which indicated that t_L was decreased with increasing amount of oil and/or S_{mix}. This might be attributed to reduction in globule size with increase in oil amount and alteration of diffusivity with increase in surfactant and cosurfactant amounts [16, 17]. However, unlike the previous two responses (Y_1 and Y_2) coefficient b_3 was found to be insignificant ($P>0.05$) with Y_3 which suggest that amount of water (X_3) had not significantly contributed for lag time of LDPH loaded MEs.

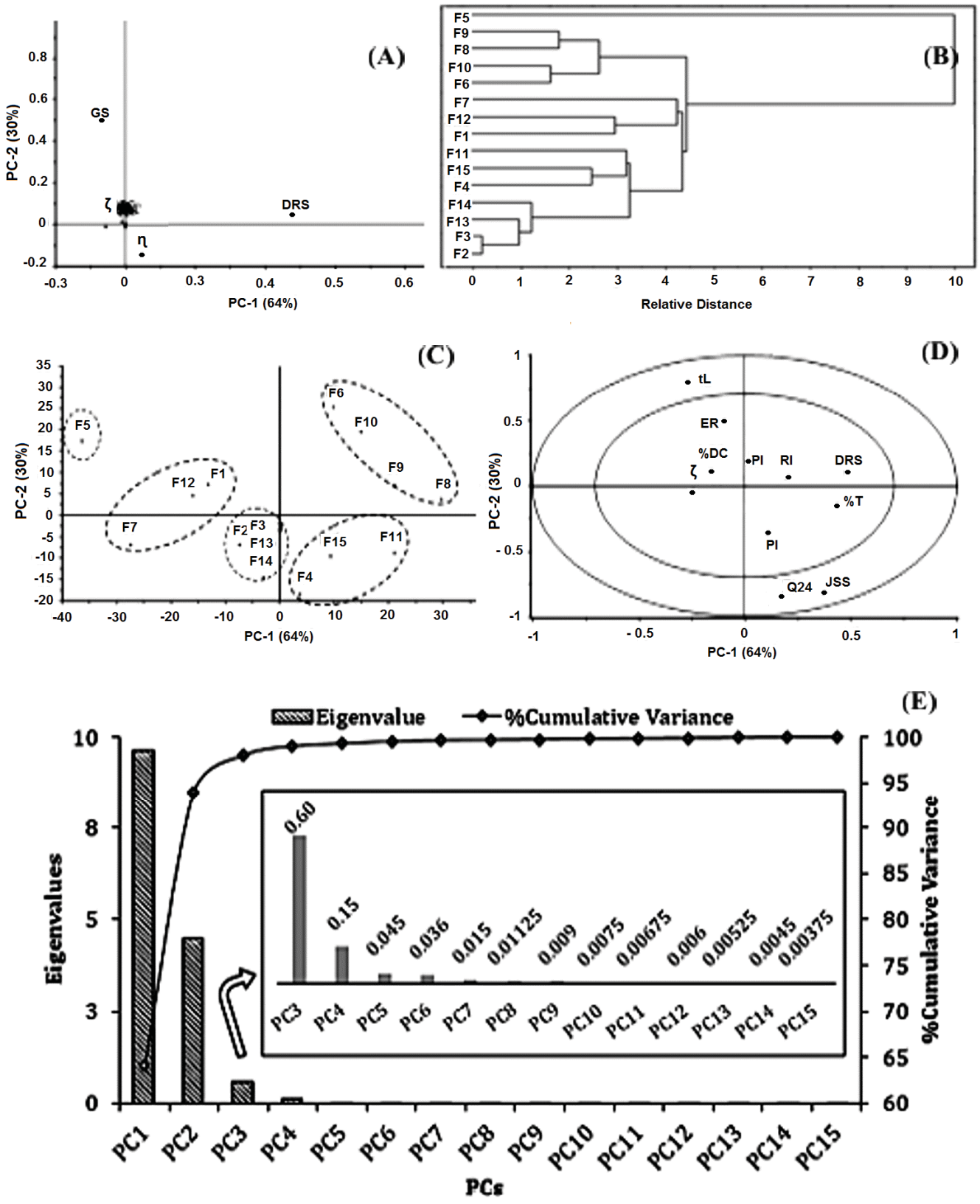

Fig. (2). PCA plots of LDPH loaded MEs (**A**) Loading plot from PCA (**B**) Dendrogram from AHCA (**C**) Scoring plot from PCA (**D**) Correlation loading plot from PCA (**E**) Scree plot from PCA.

Table 3 (i). Results of Central Composite Design Batches of LDPH Loaded MEs.

Batch Code	Globule Size (nm)	PI[a]	ζ [b] (mV)	RI [c]	%T [d]	%DC [e]	[f] (cps)
LDPH-ME-F1	89.24 ± 5.24	0.23 ± 0.06	30.47 ± 1.04	1.45 ± 0.06	99.45 ± 0.45	100.35 ± 0.26	28.53 ± 1.34
LDPH-ME-F2	77.26 ± 6.15	0.18 ± 0.07	46.25 ± 3.60	1.38 ± 0.06	100.09 ± 0.53	101.35 ± 0.13	24.14 ± 1.45
LDPH-ME-F3	78.26 ± 7.15	0.15 ± 0.05	45.25 ± 4.65	1.49 ± 0.03	101.34 ± 0.67	99.67 ± 0.65	23.26 ± 1.14
LDPH-ME-F4	67.26 ± 6.65	0.14 ± 0.06	34.33 ± 2.56	1.47 ± 0.07	98.56 ± 0.22	98.15 ± 0.14	29.35 ± 1.75
LDPH-ME-F5	98.14 ± 5.57	0.13 ± 0.04	42.67 ± 3.04	1.46 ± 0.03	97.98 ± 0.76	101.35 ± 0.33	18.36 ± 1.09
LDPH-ME-F6	110.46 ± 8.57	0.17 ± 0.05	38.32 ± 2.65	1.49 ± 0.07	99.35 ± 0.78	99.00 ± 0.20	20.14 ± 1.14
LDPH-ME-F7	75.26 ± 5.22	0.15 ± 0.03	45.25 ± 3.07	1.41 ± 0.06	100.00 ± 0.15	100.04 ± 0.45	22.78 ± 1.65
LDPH-ME-F8	89.00 ± 7.23	0.11 ± 0.02	39.14 ± 2.14	1.48 ± 0.04	101.00 ± 0.65	101.57 ± 0.14	16.00 ± 1.65
LDPH-ME-F9	93.14 ± 4.14	0.17 ± 0.06	41.65 ± 3.14	1.36 ± 0.08	100.23 ± 0.16	100.56 ± 0.65	19.45 ± 1.65
LDPH-ME-F10	103.45 ± 9.19	0.19 ± 0.04	41.14 ± 3.14	1.45 ± 0.04	99.98 ± 0.65	98.36 ± 0.16	20.22 ± 1.33
LDPH-ME-F11	77.25 ± 6.15	0.17 ± 0.07	36.37 ± 2.33	1.47 ± 0.07	99.40 ± 0.40	99.47 ± 0.56	21.35 ± 1.67
LDPH-ME-F12	86.14 ± 5.57	0.14 ± 0.02	39.68 ± 2.67	1.39 ± 0.03	98.36 ± 0.33	98.90 ± 0.16	20.15 ± 1.08
LDPH-ME-F13	77.37 ± 5.33	0.16 ± 0.04	40.00 ± 2.76	1.45 ± 0.05	100.34 ± 0.67	100.00 ± 0.65	19.57 ± 1.30
LDPH-ME-F14	69.26 ± 5.14	0.15 ± 0.05	42.42 ± 4.23	1.44 ± 0.04	99.72 ± 0.14	99.46 ± 0.76	19.25 ± 1.45
LDPH-ME-F15	76.45 ± 5.27	0.16 ± 0.03	40.14 ± 3.14	1.46 ± 0.03	99.34 ± 0.46	99.35 ± 0.15	28.14 ± 1.65

The results are of mean ± SD (n=3), [a] PI: Polydispersibility index, [b] ζ: Zeta potential, [c] RI: Refractive index, [d] %T: Percentage transmittance, [e] %DC: Percentage drug content, [f] η: Viscosity.

Table 3 (ii). Results of Central Composite Design Batches of LDPH Loaded MEs.

Batch Code	Q_{24} [a] (mg/cm^2)	J_{ss} [b] (mg/cm^2h)	t_L [c] (h)	ER [d]	K_p [e] X 10^{-2}	%DRS [f]
LDPH-ME-F1	3036.25 ± 105.25	140.57 ± 21.35	0.65 ± 0.04	2.18 ± 0.03	1.41 ± 0.34	90.00 ± 6.50
LDPH-ME-F2	3143.35 ± 135.56	150.56 ± 23.14	0.55 ± 0.09	2.34 ± 0.08	1.51 ± 0.45	98.47 ± 7.50
LDPH-ME-F3	4000.43 ± 156.14	190.42 ± 23.65	0.38 ± 0.06	2.96 ± 0.07	1.91 ± 0.14	100.47 ± 5.57
LDPH-ME-F4	4141.15 ± 125.65	198.34 ± 27.36	0.34 ± 0.06	3.08 ± 0.06	1.98 ± 0.45	110.00 ± 7.45
LDPH-ME-F5	3301.09 ± 123.65	150.14 ± 15.56	0.59 ± 0.07	2.33 ± 0.05	1.50 ± 0.13	67.26 ± 6.53
LDPH-ME-F6	3523.15 ± 122.00	157.57 ± 17.30	0.53 ± 0.08	2.45 ± 0.07	1.58 ± 0.34	112.46 ± 8.56
LDPH-ME-F7	4216.25 ± 190.14	200.35 ± 21.14	0.33 ± 0.04	3.11 ± 0.05	2.00 ± 0.16	78.37 ± 5.14
LDPH-ME-F8	4443.65 ± 198.13	207.35 ± 25.50	0.30 ± 0.07	3.22 ± 0.06	2.07 ± 0.54	134.16 ± 8.14
LDPH-ME-F9	3635.65 ± 145.54	160.00 ± 13.56	0.49 ± 0.08	2.49 ± 0.08	1.62 ± 0.14	125.37 ± 6.36
LDPH-ME-F10	3737.54 ± 165.24	169.00 ± 18.34	0.45 ± 0.04	2.63 ± 0.03	1.69 ± 0.15	118.68 ± 7.62
LDPH-ME-F11	3066.25 ± 105.09	139.68 ± 15.90	0.68 ± 0.08	2.17 ± 0.02	1.40 ± 0.17	126.45 ± 7.14
LDPH-ME-F12	4512.14 ± 175.45	220.34 ± 23.33	0.27 ± 0.06	3.42 ± 0.06	2.20 ± 0.16	88.00 ± 5.76
LDPH-ME-F13	3912.14 ± 178.70	175.32 ± 20.54	0.43 ± 0.05	2.72 ± 0.04	1.75 ± 0.14	104.26 ± 7.35
LDPH-ME-F14	4091.24 ± 201.00	180.25 ± 20.67	0.45 ± 0.02	2.80 ± 0.04	1.80 ± 0.18	103.15 ± 7.56
LDPH-ME-F15	4124.90 ± 205.23	187.25 ± 20.09	0.46 ± 0.05	2.91 ± 0.05	1.87 ± 0.24	115.16 ± 6.14

The results are of mean ± SD (n=3), [a] Q_{24}: Cumulative amount of drug permeated, [b] J_{ss}: Flux, [c] t_L: Lag time, [d] ER: Enhancement ratio, [e] K_p: Permeability coefficient, [f] DRS: Drug retained in skin.

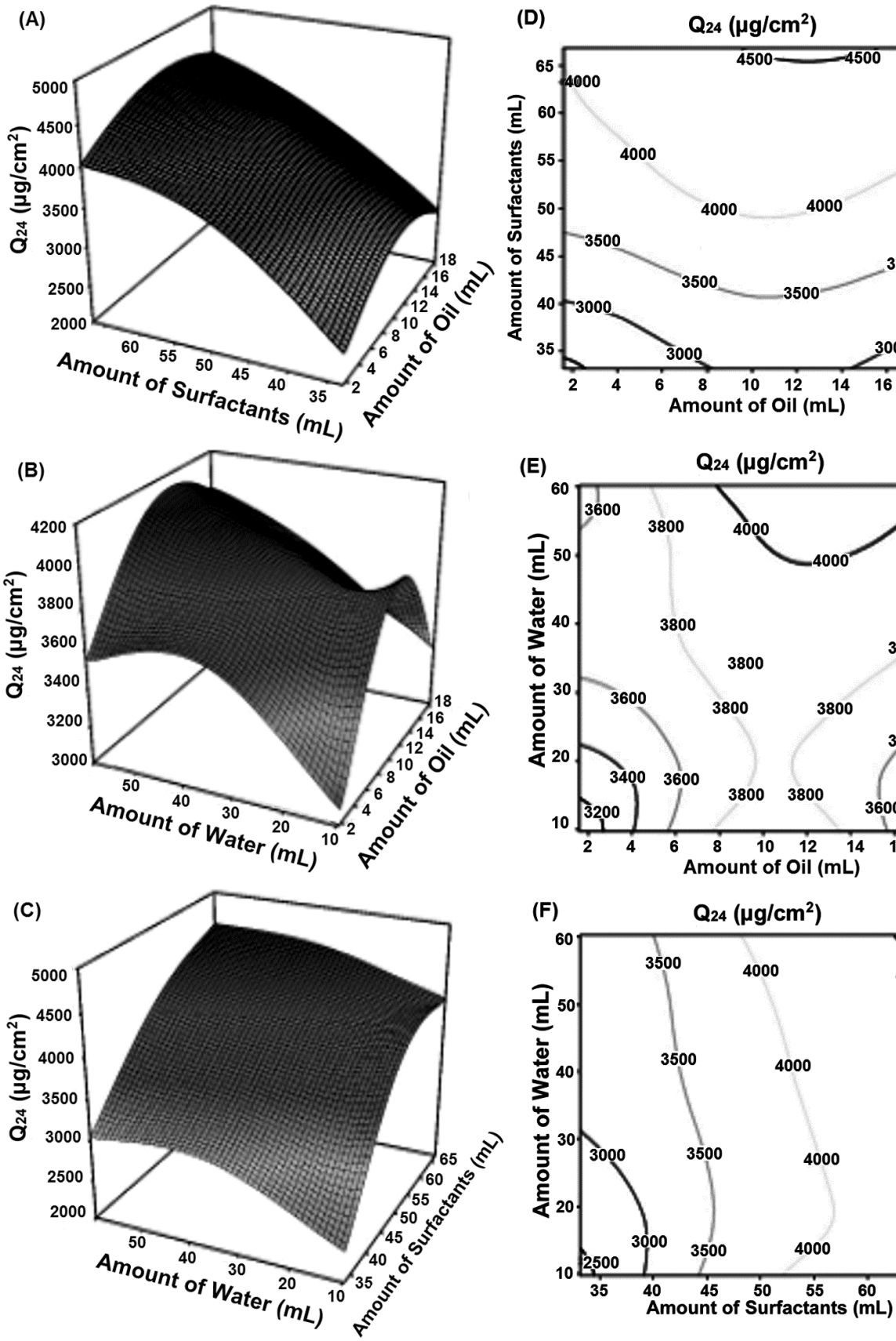

Fig. 3(i). Influence of formulation factors on Q_{24} (Y_1) of LDPH loaded MEs by response surface plots (**A**) Effect of X_1 and X_2, (**B**) Effect of X_1 and X_3, (**C**) Effect of X_2 and X_3 and contour plots (**D**) Effect of X_1 and X_2, (**E**) Effect of X_1 and X_3, (**F**) Effect of X_2 and X_3.

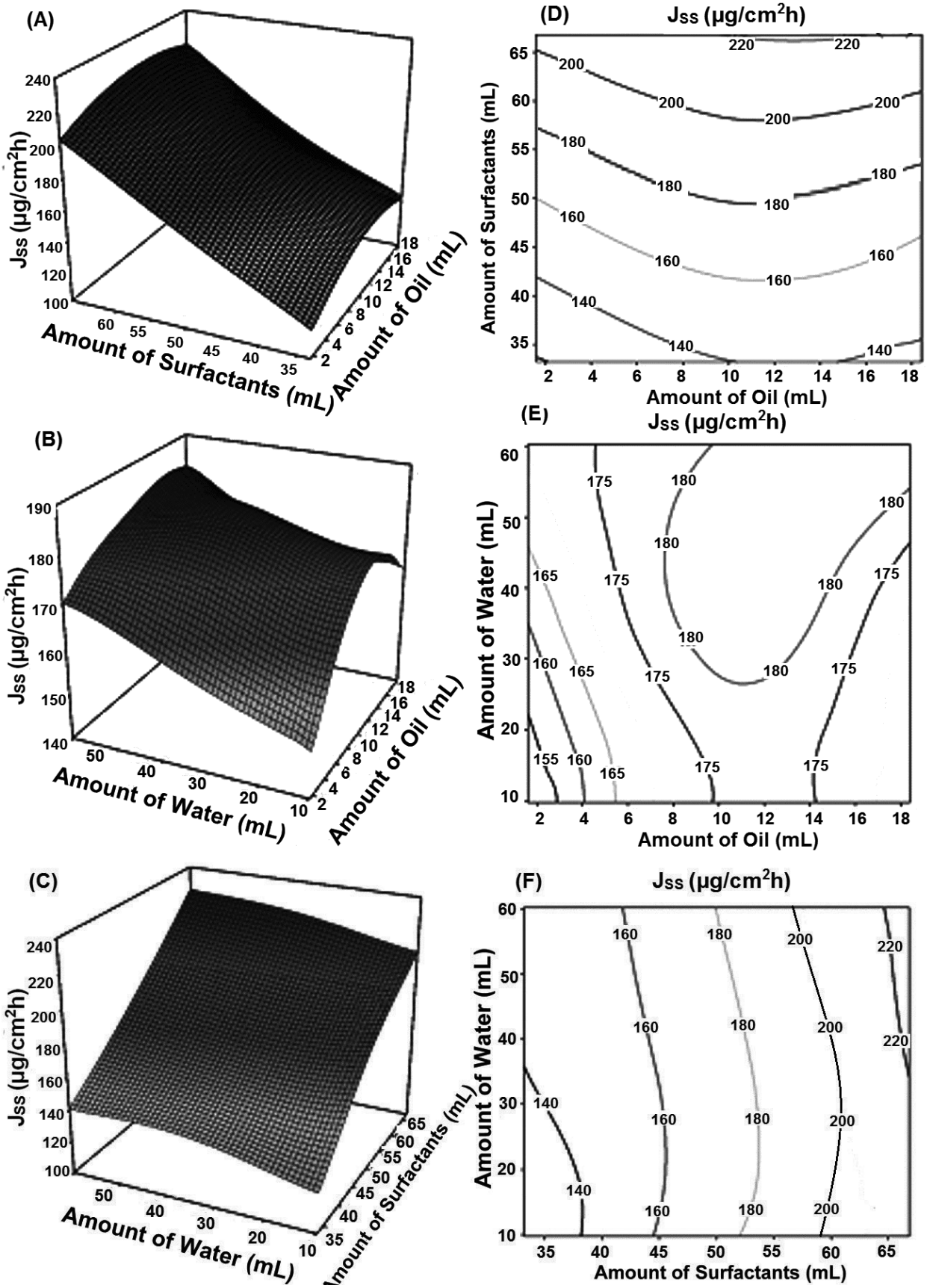

Fig. 3(ii). Influence of formulation factors on J_{ss} (Y_2) of LDPH loaded MEs by response surface plots (**A**) Effect of X_1 and X_2, (**B**) Effect of X_1 and X_3, (**C**) Effect of X_2 and X_3 and contour plots (**D**) Effect of X_1 and X_2, (**E**) Effect of X_1 and X_3, (**F**) Effect of X_2 and X_3.

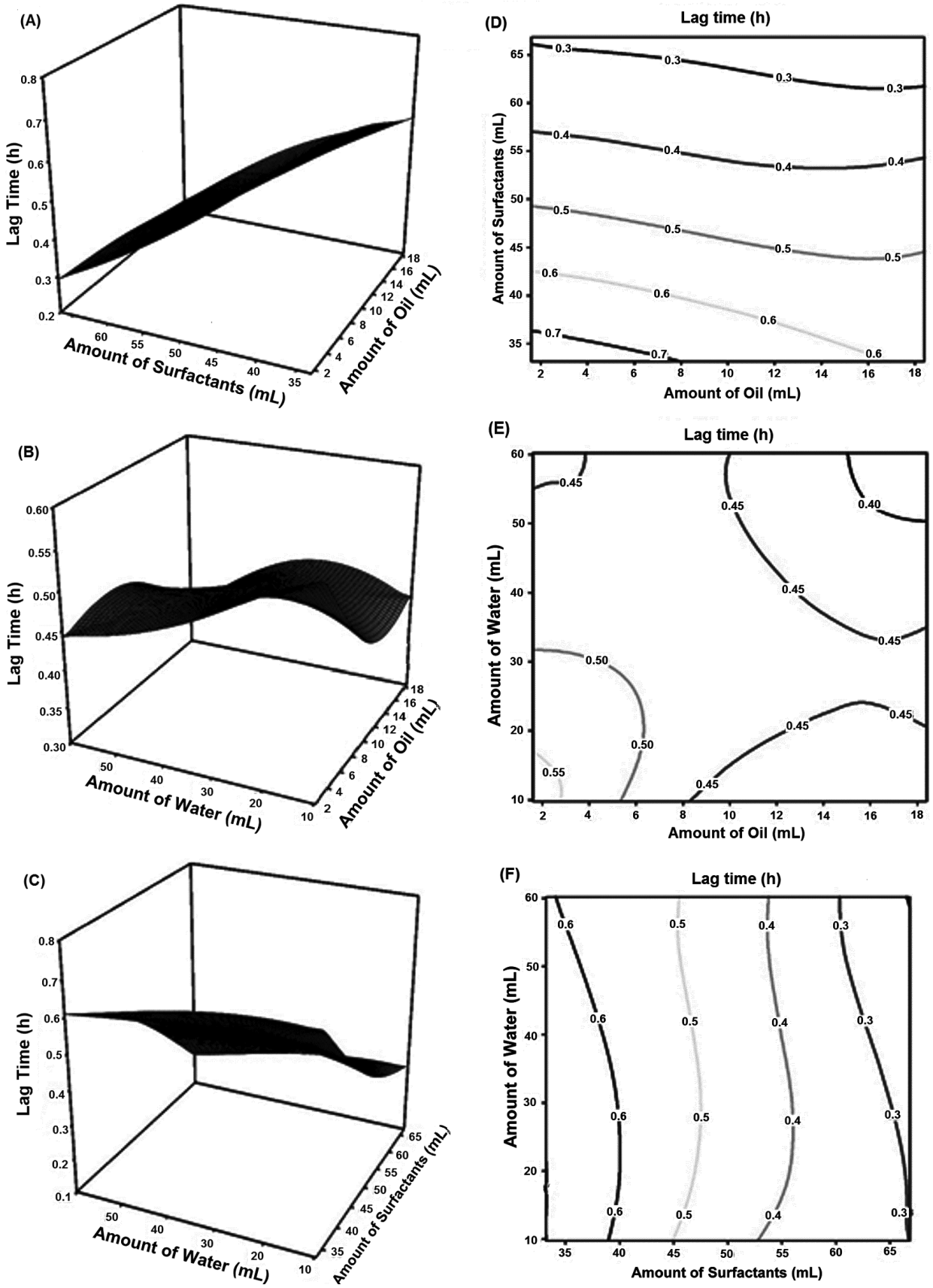

Fig. 3(iii). Influence of formulation factors on lag time (Y_3) of LDPH loaded MEs by response surface plots (**A**) Effect of X_1 and X_2, (**B**) Effect of X_1 and X_3, (**C**) Effect of X_2 and X_3 and contour plots (**D**) Effect of X_1 and X_2, (**E**) Effect of X_1 and X_3, (**F**) Effect of X_2 and X_3.

Table 4. Formulation Composition and Results of Check Point Batch for LDPH Loaded MEs.

Type of Component		Name of Component	Amount (mL)	Concentration (%w/w)
Oil (X_1)		Capryol 90	12.13	11.40
Surfactant Mixture (X_2)	Surfactant	Cremophor EL	39.38	37.04
	Cosurfactant	Ethanol	19.74	18.56
Water (X_3)		Distilled water	35	32.91
Responses	**Predicted Value**	**Experimental Value [a]**		**% Relative Error**
Q_{24} (Y_1)	4430.07 μg/cm^2	4327.20 ± 187.67 μg/cm^2		2.32
J_{ss} (Y_2)	207.67 μg/cm^{2}h	200.23 ± 12.33 μg/cm^{2}h		3.67
t_L (Y_3)	0.3387 h	0.3456 ± 0.07 h		2.03

[a] The results are of mean ± SD (n=3).

3.3.5. Model Validation and Selection of Optimized Batch

On the basis of maximum value of Q_{24} and J_{ss} along with lowest values of t_L criteria the check point/optimized batch of LDPH loaded ME was constructed practically according to the levels of factors illustrated in Table **4**. The results depicted nonsignificant ($P > 0.05$) difference and lower % relative error between experimentally obtained and theoretically computed data of all three responses (Q_{24}, J_{ss} and t_L) which suggested suitability of design applied.

3.4. Evaluation Parameters Drug Loaded MEs

3.4.1. Globule Size and Size Distribution

The globule size of the optimized batch of LDPH loaded ME was found to be 67 nm which confirmed nanometer size of developed formulation. The PI of the optimized batch of LDPH loaded ME was found to be 0.12 which illustrated narrow size distribution of developed formulation [10, 11].

3.4.2. Zeta Potential (ζ)

The ζ value of the optimized batch of LDPH loaded ME was found to be - 40.12 mV. All the values of zeta potential were higher than |30 mV| which supported stability of dispersed systems [45].

3.4.3. Refractive Index (RI)

The results of RI for all batches of experimental design for drug loaded MEs confirmed isotropic nature of the systems [17-19]. The RI value of the optimized batch of LDPH loaded ME was found to be 1.45.

3.4.4. Percentage Transmittance (%T)

In order to characterize isotropic nature of MEs, transmittance study was conducted [18, 19]. The data illustrated nearly 100% transmittance for all batches. The %T value of the optimized batch of LDPH loaded ME was found to be 99.67.

3.4.5. Percentage Drug Content

The values of percentage drug content were almost 100% along with very low standard deviations, suggested uniform dispersion of LDPH in developed formulations [52]. The value of percentage drug content for the optimized batch of LDPH loaded ME was found to be 100.12.

3.4.6. Viscosity

The viscosity of ME is crucial in terms of their ability for penetration through skin bilayers. There are reports indicating that O/W type MEs having lower values of viscosity with Newtonian-type of flow behavior [53]. The viscosity of the optimized batch of LDPH loaded ME was found to be 25.58 cps at 25°C.

3.4.7. In vitro Permeation

The results of permeation profile of all batches exhibited significant enhancement in *in vitro* permeation by MEs compared to their aqueous suspension (control) ($P < 0.05$) [22, 53]. The optimized batch of LDPH loaded ME also exhibited significant enhancement ($P < 0.05$) in all studied permeability parameters as compared to control formulation (Fig. **4**(**A**)).

3.4.8. Thermodynamic Stability

The study revealed excellent stability of optimized batch of LDPH loaded ME with no signs of phase separation or precipitation at various stress conditions studied [10].

3.4.9. Transmission Electron Microscopy

Morphological and structural examination of the optimized batch of LDPH loaded ME was carried out using transmission electron microscope. TEM images illustrated formation of spherical micelles with size range of 10 - 100 nm (Fig. **5**). These results were in accordance to that of globule size analysis and in accordance to the previous reports of ME based TDDS [21-23].

3.5. Selection of Thickening Agent

Various gelling agents were evaluated for the gelling of optimized batch of LDPH loaded ME. It was observed that sodium alginate affected the structure of the ME and resulted in separation of oily phase [38-41]. Methocel K4M and Poloxamer 188 were unable to yield viscosity desirable for the gel formulation. Further, the results revealed that only 1% w/v of Carbopol 940 concentration provided suitable viscosity to drug loaded MBG formulations. Hence, 1% w/v

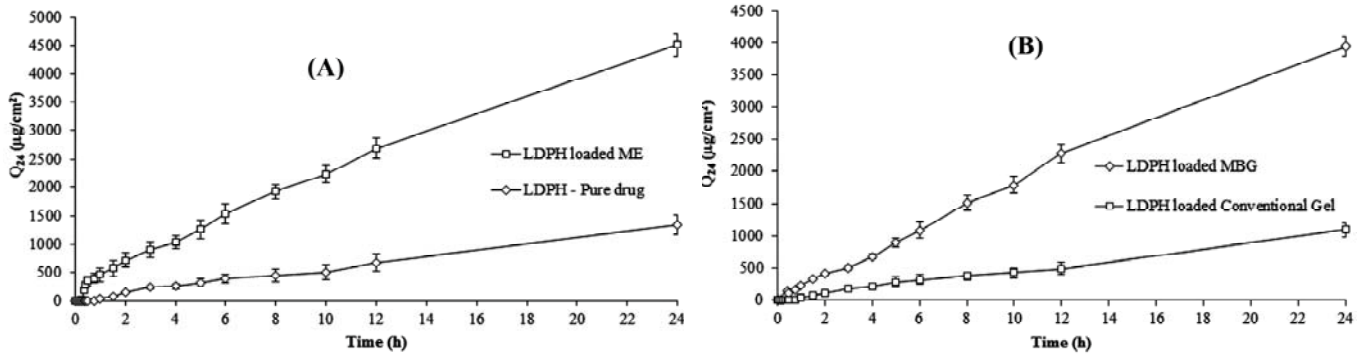

Fig. (4). Comparison of *in vitro* drug permeation profiles of (**A**) optimized batch of LDPH loaded ME against pure drug and (**B**) optimized batch of LDPH laded MBG against conventional gel, Error bar represents SD (n=3).

Carbopol 940 was selected as thickening agent for the formulation of LDPH loaded MBG.

3.6. Evaluation Parameters of LDPH Loaded O/W Type MBGs

3.6.1. Appearance

The optimized batch of drug loaded MBG was almost transparent, homogeneous and consistent along with no signs of phase separation for 24 h [40].

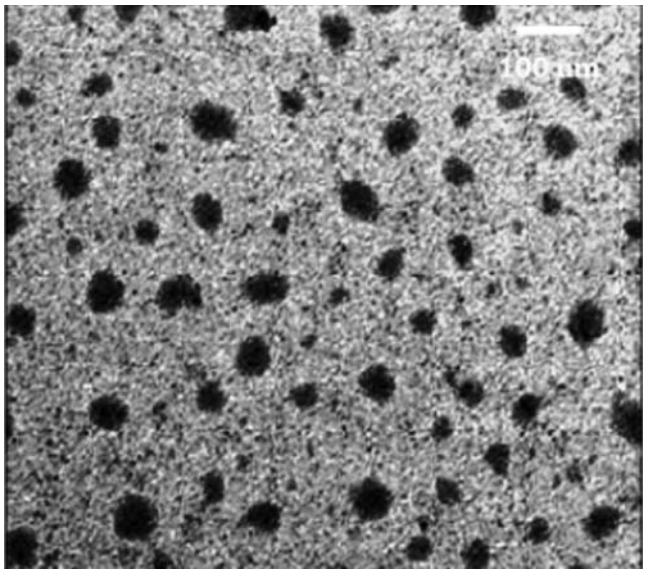

Fig. (5). TEM image of optimized batch of LDPH loaded ME.

3.6.2. Globule Size and Size Distribution

The data illustrated no significant difference ($P < 0.05$) in the values of globule size and PI of LDPH loaded MBG which conformed that inspite of conversation of liquid formulation (ME) into a semisolid form (MBG) the globule size and its distribution remains unaltered [39, 40].

3.6.3. Zeta Potential (ζ)

The data illustrated no significant difference ($P < 0.05$) in the values of ζ which conformed stability of optimized formulation inspite of conversation of liquid formulation (ME) into a semisolid form (MBG) [39].

3.6.4. pH

The value of pH for the optimized batch of LDPH loaded MBG was found to be 6.56, which was in the acceptable range for a transdermal formulation [39].

3.6.5. Viscosity

The optimized batch of LDPH loaded MBG showed pseudo-plastic behavior with the value of viscosity as 189.35 cps. The enhanced viscosity for the MBG as compared to ME might be attributed to the gel formulation properties of Carbopol 934 as thickening agent [39, 40].

3.6.6. Percentage Drug Content (% DC)

The percentage drug content of the optimized batch of LDPH loaded MBG was found to be 98.36. The values of percentage drug content were almost 100% along with very low standard deviations, suggested uniform dispersion of drug in developed formulations [39].

3.6.7. In vitro Permeation

The optimized batch of LDPH loaded MBG exhibited significant enhancement ($P < 0.05$) in all studied permeability parameters as compared to its conventional gel formulation (control) (Fig. **4**(**B**)). The significantly higher values of Q_{24}, J_{ss}, K_p and lower values of t_L for the optimized batch of LDPH loaded MBG as compared to its conventional gel suggested marked improvement in diffusion rate by the developed formulations [39]. The desired input rate of LDPH was decided by calculating drug concentrations required to elicit the pharmacological effect as per following equation.

$$\text{Desired Input Rate} = C_{ss} \times C_L \times \text{B.W.} \quad (12)$$

The practical value of J_{ss} for optimized batch of LDPH loaded MBG was found to be 196.47 µg/cm^{2}h which revealed area of 7.95 cm^2 in order to match the desired input rate.

3.6.8. Skin Irritation Study

Primary skin irritation study was performed for optimized batch of LDPH loaded MBG to exclude any possibility of potential dermal irritation. A PDII of 0.0425 revealed

that the optimized formulation was non-irritant, free from skin sensitization and safe for use [42, 43].

3.6.9. Stability Study

In the present work, accelerated stability study was carried out for optimized batch of MBG at 40±2°C and 75±5% RH for six months and the results showed no remarkable change in the all selected responses [38-41].

4. CONCLUSIONS

The present investigation revealed that both rate and extend of LDPH transport across rat abdominal skin were highly dependent on the amounts of oil, surfactant, cosurfactant and water of developed formulations. The optimized batch of LDPH loaded ME comprised of 11.4% w/w of capryol 90 as oil phase, 37.04% w/w cremophor EL as surfactant, 18.56% w/w of ethanol as cosurfactant and 32.91% w/w of water exploited a mean globule size as 67 nm. The LDPH loaded ME was successfully converted into MBG by using carbopol 940 as thickening agent. The optimized batch of LDPH loaded MBG delivered LDPH with a flux value of 196.4740.69 μg/cm^{2}h in the *in vitro* skin permeation study with overall requirement of 7.95 cm^2 application area. Thus, it could be concluded from the present investigation that O/W type microemulsion could be an excellent approach for successful transdermal delivery of poorly water soluble drugs like, LDPH. However further, *in vivo* investigations are required to confirm improved antihypertensive efficacy of LDPH.

CONFLICT OF INTEREST

The authors confirm that this article content has no conflicts of interest.

ACKNOWLEDGEMENTS

We would like to thank Torrent Research Center for providing gift sample of Lercanidipine HCl.

REFERENCES

[1] Sweetman SC. Martindale - The Complete Drug Reference; Pharmaceutical Press, London, 2009.

[2] Burnier M, Pruijm M, Wuerzner G. Treatment of essential hypertension with calcium channel blockers: What is the place of lercanidipine? Exp Opin Drug Metab Toxicol 2009; 5: 981-87.

[3] Beckey C, Lundy A, Lutfi N. Lercanidipine in the treatment of hypertension. Ann Pharmacother 2007; 41: 465-73.

[4] Prausnitz MR, Langer R. Transdermal drug delivery. Nat Biotechnol 2008; 26: 1261-68.

[5] Joonho C, Min-Koo C, Saeho C, *et al.* Effect of fatty acids on the transdermal delivery of donepezil: *In vitro* and *in vivo* evaluation. Int J Pharm 2012; 422: 83-90.

[6] Biana G, Elka T. Transdermal skin delivery: Predictions for humans from *in vivo*, *ex vivo* and animal models. Adv Drug Deliv Rev 2007; 59: 1152-61.

[7] Marie-Alexandrine B, Stéphanie B, Jocelyne P, *et al.* Penetration of drugs through skin, a complex rate-controlling membrane. Curr Opin Colloid Interface Sci 2012; 17: 156-65.

[8] Kiyomi W, Takuya H, Kenjirou Y, *et al.* An insight into the role of barrier related skin proteins. Int J Pharm 2012; 427: 293-98.

[9] Barry BW. Drug delivery routes in skin: A novel approach. Adv Drug Deliv Rev 2002; 54: 31-40.

[10] Date AA, Patravale VB. Microemulsions: Applications in transdermal and dermal delivery. Crit Rev Ther Drug Carrier Syst 2007; 24: 547-96.

[11] Fanun M. Microemulsions: Properties and Applications, Surfactant Science Series, Taylor and Francis, CRC Press, Boca Raton, 2009.

[12] Bagwe RP, Kanicky JR, Palla BJ, *et al.* Improved drug delivery using microemulsions: rationale, recent progress, and new horizons. Crit Rev Ther Drug Carrier Syst 2001; 18: 77-140.

[13] Barot BS, Parejiya PB, Patel HK, *et al.* Microemulsion-based gel of terbinafine for the treatment of onychomycosis: Optimization of formulation using D-optimal design. AAPS Pharm Sci Tech 2012; 13: 184-91.

[14] Derle DV, Sagar BSH, Pimpale R. Microemulsion as a vehicle for transdermal permeation of nimesulide. Ind J Pharm Sci 2006; 68: 622-25.

[15] Bekir GM, Haluk H, Stephanie RD. One-step separation of β-galactosidase from β-lactoglobulin using water-in-oil microemulsions. Food Chemistry 2012; 132: 326-32.

[16] Abood RM, Talegaonkar S, Tariq M, *et al.* Microemulsion as a tool for the transdermal delivery of ondansetron for the treatment of chemotherapy induced nausea and vomiting. Colloids Surf B 2013; 101: 143-51.

[17] Xiao Y, Liu F, Ping Q, *et al.* The influence of the structure and the composition of water/AOT-Tween 85/IPM microemulsion system on transdermal delivery of 5-fluorouracil. Drug Dev Ind Pharm 2012; 38: 1521-29.

[18] Azeem A, Rizwan M, Ahmad FJ, *et al.* Nanoemulsion components screening and selection: a technical note. AAPS Pharm Sci Tech 2009; 10: 69-76.

[19] Shafiq-un-Nabi S, Shakeel F, Talegaonkar S, *et al.* Formulation development and optimization using nanoemulsion technique: A technical note. AAPS Pharm Sci Tech 2007; 8: 1-6.

[20] Kumar P, Mittal KL. Handbook of Microemulsion Science and Technology, Marcel Dekker, New York, 1999.

[21] Shakeel F, Ramadan W, Ahmed MA. Investigation of true nanoemulsions for transdermal potential of indomethacin: Characterization, rheological characteristics, and *ex vivo* skin permeation studies. J Drug Target 2009; 17: 435-41.

[22] Okur NU, Apaydın S, Yavaşoğlu NK, *et al.* Evaluation of skin permeation and anti-inflammatory and analgesic effects of new Naproxen microemulsion formulations. Int J Pharm 2011; 416: 136-44.

[23] Zhang J, Michniak-Kohn B. Investigation of microemulsion microstructures and their relationship to transdermal permeation of model drugs: Ketoprofen, lidocaine and caffeine. Int J Pharm 2011; 421: 34-44.

[24] Po-Hsien L, Been-Huang C. Process optimization and stability of D-limonene-in-water nanoemulsions prepared by ultrasonic emulsification using response surface methodology. Ultrason Sonochem 2012; 19: 192-97.

[25] Peng-Fei Y, Qin Z, Mei-Xiang L, *et al.* Process optimization, characterization, and release study *in vitro* of an intravenous puerarin lipid microspheres loaded with the phospholipid complex. J Dispersion Sci Technol 2011; 32: 1-10.

[26] Garala K, Patel J, Patel A, *et al.* Enhanced encapsulation of metoprolol tartrate with carbon nanotubes as adsorbent. Appl Nanosci 2011; 1: 219-30.

[27] Kaul G, Huang J, Chatlapalli R, *et al.* Quality-by-design case study: Investigation of the role of poloxamer in immediate-release tablets by experimental design and multivariate data analysis. AAPS Pharm Sci Tech 2011; 12: 1064-76.

[28] Zidan AS, Mokhtar M. Multivariate optimization of formulation variables influencing flurbiprofen proniosomes characteristics. J Pharm Sci 2011; 100: 2212-21.

[29] Singh B, Kumar R, Ahuja N. Optimizing drug delivery systems using systematic "design of experiments." Part I: fundamental aspects. Crit Rev Ther Drug Carrier Syst 2005; 22: 27-105.

[30] Singh SK, Ranja P, Verma P, *et al.* Glibenclamide-loaded self-nanoemulsifying drug delivery system: Development and characterization. Drug Dev Ind Pharm 2010; 6: 933-45.

[31] Patel MR, Patel RB, Parikh JR, *et al.* Effect of formulation components on the *in vitro* permeation of microemulsion drug delivery system of fluconazole. AAPS Pharm Sci Tech 2009; 10: 917-23.

[32] Hathout RM, Woodman TJ, Mansour S, *et al.* Microemulsion formulations for the transdermal delivery of testosterone. Eur J Pharm Sci 2010; 40: 188-96.

[33] Ming K, Xi GC, Dong KK, *et al.* Investigations on skin permeation of hyaluronic acid based nanoemulsion as transdermal carrier. Carbohydr Polymer 2011; 86: 837- 43.

[34] Banweer J, Pandey S, Pathak AK. Development and optimization of transdermal system of lisinopril dehydrate: Employing permeation enhancers. Iranian J Pharm Sci 2010; 6: 245-51.

[35] Roberta C, Valentina M, Ela H, *et al.* Permeation and skin retention of quercetin from microemulsions containing Transcutol P. Drug Dev Ind Pharm 2012; 38: 1128-33.

[36] Ganguly R, Choudhury N. Investigating the evolution of the phase behavior of AOT-based w/o microemulsions in dodecane as a function of droplet volume fraction. J Colloid Interface Sci 2012; 372: 45-51.

[37] Lorena T, Pasquale A, Rita M, *et al.* Niosomes vs microemulsions: New carriers for topical delivery of capsaicin. Colloids Surf B 2011; 87: 333-39.

[38] Hashem FM, Shaker DS, Ghorab MK, *et al.* Formulation, characterization, and clinical evaluation of microemulsion containing clotrimazole for topical delivery. AAPS Pharm Sci Tech 2011; 12: 879-86.

[39] Heard CM, Kung D, Thomas CP. Skin penetration enhancement of mefenamic acid by ethanol and 1,8-cineole can be explained by the 'pull effect'. Int J Pharm 2006; 321: 167-70.

[40] Branka R, Mirjam G, Mirjana G, *et al.* Dual influence of colloidal silica on skin deposition of vitamins C and E simultaneously incorporated in topical microemulsions. Drug Dev Ind Pharm 2010; 36: 852-60.

[41] Branka R, Alenka Z, Francoise F, *et al.* Temperature-sensitive microemulsion gel: An effective topical delivery system for simultaneous delivery of vitamins C and E. AAPS Pharm Sci Tech 2009; 10: 54-61.

[42] Bachhav YG, Patravale VB. Microemulsion based vaginal gel of fluconazole: Formulation, *in vitro* and *in vivo* evaluation. Int J Pharm 2009; 365: 175-79.

[43] Weiwei Z, Chenyu G, Aihua Y, *et al.* Microemulsion-based hydrogel formulation of penciclovir for topical delivery. Int J Pharm 2009; 378: 152-58.

[44] Draize JH, Woodard G, Calvery HO. Methods for the study of irritation and toxicity of substances applied to the skin and mucous membranes. J Pharmacol Exp Ther 1944; 82: 377-90.

[45] Gannu R, Palem CR, Yamsani VV, *et al.* Enhanced bioavailability of lacidipine via microemulsion based transdermal gels: Formulation optimization, *ex vivo* and *in vivo* characterization. Int J Pharm 2010; 388: 231-41.

[46] Darole PS, Hegde DD, Nair HA. Formulation and evaluation of microemulsion based delivery system for amphotericin B. AAPS Pharm Sci Tech 2008; 9: 122-28.

[47] Lawrence MJ, Rees GD. Microemulsion-based media as novel drug delivery systems. Adv Drug Del Rev 2000; 45: 89-121.

[48] Borhade V, Pathak S, Sharma S, *et al.* Clotrimazole nanoemulsion for malaria chemotherapy. Part II: Stability assessment, *in vivo* pharmacodynamic evaluations and toxicological studies. Int J Pharm 2012; 431: 138-48.

[49] Ringnér M. What is principal component analysis? Nat Biotechnol 2008; 26: 303-04.

[50] Rajalahti T, Kvalheim OM. Multivariate data analysis in pharmaceutics: A tutorial review. Int J Pharm 2011; 417: 280-90.

[51] Martins S, Tho I, Souto E, *et al.* Multivariate design for the evaluation of lipid and surfactant composition effect for optimization of lipid nanoparticles. Eur J Pharm Sci 2012; 45: 613-623.

[52] Kubista M, Sjögreen B, Forootan A, *et al.* Real-time PCR gene expression profiling. Eur Pharm Rev 2007; 1: 56-60.

[53] Dai X, Moffat JG, Wood J, *et al.* Thermal scanning probe microscopy in the development of pharmaceuticals. Adv Drug Del Rev 2012; 64: 449-60.

[54] Yating F, Xinru L, Yanxia Z, *et al.* Improved intestinal delivery of salmon calcitonin by water-in-oil microemulsions. Int J Pharm 2011; 416: 323-30.

Received: August 08, 2013 Revised: September 19, 2013 Accepted: October 01, 2013